

Le sfide
più grandi.
La scienza
più avanzata.

abbvie

Siamo impegnati nel rispondere alle sfide più grandi in tema di salute.

Mettiamo in campo innovazione e passione, dove il bisogno è maggiore.

Come azienda biofarmaceutica globale, il nostro obiettivo è avere un impatto significativo sulla vita delle persone.


È con il contributo di tutti che i progressi della scienza si traducono in farmaci per milioni di persone. Per questo collaboriamo con università e centri di ricerca, organizzazioni governative, associazioni di pazienti e no profit.

Insieme, costruiamo la medicina del futuro.

abbvie.it

People. Passion.
Possibilities.®

Rapamycin promotes autophagy cell death of Kaposi's sarcoma cells through P75^{NTR} activation

Simona Lupinacci¹ | Anna Perri¹  | Giuseppina Toteda¹ | Donatella Vizza¹ | Danilo Lofaro¹ | Paola Pontrelli² | Giovanni Stallone³ | Chiara Divella² | Gianpaolo Tessari⁴ | Antonella La Russa¹ | Gianluigi Zaza⁵ | Renzo Bonfiglio¹

¹Department of Nephrology, Dialysis and Transplantation, "Kidney and Transplantation" Research Centre, Annunziata Hospital, Cosenza, Italy

²Nephrology Unit, Department of Emergency and Organ Transplantation, University of Bari Aldo Moro, Bari, Italy

³Nephrology Dialysis and Transplantation Unit, Department of Medical and Surgical Sciences, University of Foggia, Foggia, Italy

⁴Section of Dermatology and Venereology, University-Hospital of Verona, Verona, Italy

⁵Renal Unit, Department of Medicine, University-Hospital of Verona, Verona, Italy

Correspondence

Anna Perri, Department of Nephrology, Dialysis and Transplantation, "Kidney and Transplantation" Research Centre, Annunziata Hospital, Cosenza, Italy.
Email: perria71@gmail.com

Abstract

The mammalian target of rapamycin inhibitor (mTOR-I) Rapamycin, a drug widely used in kidney transplantation, exerts important anti-cancer effects, particularly in Kaposi's Sarcoma (KS), through several biological interactions. In this in vivo and in vitro study, we explored whether the activation of the autophagic pathway through the low-affinity receptor for nerve growth factor, p75^{NTR}, may have a pivotal role in the anti-cancer effect exerted by Rapamycin in S. Our Immunohistochemistry results revealed a significant hyper-activation of the autophagic pathway in KS lesions. In vitro experiments on KS cell lines showed that Rapamycin exposure reduced cell viability by increasing the autophagic process, in the absence of apoptosis, through the transcriptional activation of p75^{NTR} via EGR1. Interestingly, p75^{NTR} gene silencing prevented the increase of the autophagic process and the reduction of cell viability. Moreover, p75^{NTR} activation promoted the upregulation of phosphatase and tensin homolog (PTEN), a tumour suppressor that modulates the PI3K/Akt/mTOR pathway. In conclusion, our in vitro data demonstrated, for the first time, that in Kaposi's sarcoma, autophagy triggered by Rapamycin through p75^{NTR} represented a major mechanism by which mTOR inhibitors may induce tumour regression. Additionally, it suggested that p75^{NTR} protein analysis could be proposed as a new potential biomarker to predict response to Rapamycin in kidney transplant recipients affected by Kaposi's sarcoma.

KEYWORDS

Beclin-1, EGR1, PI3K/Akt/mTOR pathway, PTEN

1 | INTRODUCTION

Kaposi's sarcoma (KS) is a multifocal angio-proliferative neoplasm frequently affecting immunosuppressed patients, which incidence is greatly increased in renal transplant recipients compared with the general population, with particular prevalence in certain ethnic

groups where it can occur in up to 5% of transplant recipients.¹⁻³ The increased incidence of KS in transplant populations may, in part, be attributed to the choice of immunosuppressive regimen with calcineurin inhibitor (CNI)-based immunosuppression being associated with the development of the tumour.^{4,5} On the contrary, literature evidence reports that mammalian target of rapamycin inhibitors

Simona Lupinacci and Anna Perri contributed equally to the work.

© 2021 John Wiley & Sons A/S. Published by John Wiley & Sons Ltd

(mTOR-Is) may have curative effects, as clinical studies have demonstrated that conversion to mTOR-Is along with the concomitant withdrawal of CNIs may lead to a rapid resolution of cutaneous Kaposi's lesion.^{6,7}

The aforementioned mTOR-Is anti-proliferative effects seem to be related to their ability to inhibit the PI3K/Akt/mTOR pathway, an intracellular signalling pathway regulating cell cycle, proliferation, survival, mobility and angiogenesis of tumour cells. Additionally, as recently reported, mTOR-I-induced autophagy may potentiate these effects.⁸

Autophagy is a lysosomal catabolic process that maintains cellular homeostasis by degrading damaged intracellular organelles and cytoplasmic components; such degradation is critical for cell survival under unfavourable growth conditions, such as energy deprivation.⁹ However, in cancer, this process can be considered "a double edge sword," since it can either counteract or promote cell death, depending on the different cancer cell types and conditions.^{10,11} Despite the proven efficacy of Rapamycin in promoting autophagy in cancer, the underlying molecular mechanism is not yet well understood.

Recently, we reported that in tubular renal cells exposed to albumin overload, Rapamycin treatment activates the autophagic flux through the transcriptional activation of the p75^{NTR},¹² a low-affinity receptor for nerve growth factor. The biological effects of p75^{NTR} are cell-type dependent and include survival, apoptosis, migration, differentiation, (pro)-neurotrophin binding, interacting transmembrane coreceptor expression, intracellular adaptor molecule availability and post-translational modifications.¹³ Interestingly, in the last few years, exciting reports have emerged regarding the role of p75^{NTR} in many cancer types, demonstrating that its activation elicits various biological responses by triggering quite different pathways.¹⁴

Therefore, to assess whether, similarly to other cancers, Rapamycin exerted antineoplastic effects in KS through the activation of autophagy via p75^{NTR}, we performed *in vitro* experiments, employing several laboratory techniques.

2 | METHODS

2.1 | Skin biopsies specimens

Skin biopsies of KS lesions and normal-appearing perilesional skin were performed by a trained dermatologist of the University Hospital of Verona using local anaesthesia with lidocaine 1% and then sent to the Pathology Department for histological evaluations. Biopsy specimens were fixed in 4% formaldehyde and embedded in paraffin according to standard procedures. Paraffin-embedded skin specimens were used for conventional histologic staining.

At the time of cute biopsy, all patients gave their informed consent to use remaining portions of biopsy specimens for research purpose after their primary use for routine histologic staining. Therefore, no formal ethical approval was required for processing archival cute biopsies for our study.

2.2 | Immunohistochemistry

After antigen retrieval, paraffin-embedded skin sections were permeabilized with Triton (0.25%) for 5 min and then blocked with Protein Block Solution (Dako Cytomation, Glostrup, Denmark) for 10 min. Incubation was performed with an antibody against p75^{NTR} (Santa Cruz Biotechnologies, Santa Cruz, CA) and detected by the peroxidase/DAB Dako Real EnVision Detection System (Dako). The peroxidase reaction was shown by a brown precipitate, counterstained with Mayer's hematoxylin (blue). Images were scanned by the Aperio ScanScope CS2 device (Aperio Technologies, Vista, CA).

2.3 | Confocal laser scanning microscopy

Paraffin-embedded skin sections, obtained by typical cutaneous lesions of KS and normal perilesional skin, were used for morphologic analyses by hematoxylin and eosin staining and immunohistochemical analyses for BCN1, LC3B and SQSTM1 (Santa Cruz Biotechnologies, Santa Cruz, CA) and subsequently analysed by confocal microscopy. After blocking, the slides were incubated with the primary antibodies overnight at 4°C. Negative controls were obtained by incubation with a control irrelevant antibody. The immune complex was then identified with the secondary antibody (Alexa Fluor 488, Molecular Probes, Eugene, OR). All sections were counterstained with DAPI (Molecular Probes). The specific fluorescence was analysed using the Leica TCS SP8 (Leica, Wetzlar, Germany) confocal laser-scanning microscope. Specific immunostaining was quantified using Image J software and expressed as % of positive area as previously described.¹⁵

2.4 | Cell culture and treatments

Human immortalized Kaposi Sarcoma-Immortal (KS) cells, a HHV8 negative KS cell line¹⁶ were kindly provided by Dr. A. Albini (Istituto Nazionale per la Ricerca sul Cancro, Genoa, Italy) and were cultured as described in Stallone et al.¹⁷ The cells were treated as follows: Rapamycin (Rapa—from 0.1 to 150 ng/ml; Sigma Aldrich, Missouri, USA); Bafilomycin A1 (BAF, 25 nM; Sigma Aldrich, Missouri, USA); Mithramycin A (100 nM), PD98059 (10 mM; Sigma Aldrich, Missouri, USA). In all experiments, the control was treated with DMSO (untreated, -).

2.5 | MTT assay

KS cells (5 × 10³ cells/well) grown in 96 well plates were exposed to treatments as indicated. MTT assay has been performed as previously described.¹⁸

The values for 50% inhibitory concentration (IC50) were calculated using the GraphPad software (GraphPad Software Inc., San Diego, CA).

2.6 | Soft agar assay

KS cells (2×10^4) were plated in 2 ml of 0.35% agarose with 5% FBS in phenol red-free media, in a 0.7% agarose base in 12-well plates. Two days after plating, media containing treatments were added to the top layer, and the media were replaced every 2 days. After 14 days, 150 μ l of MTT (2 mg ml^{-1}) was added to each well and allowed to incubate at 37°C for 4 h. Plates were then placed at 4°C overnight and colonies >50 μ m diameter from triplicate assays were counted.

2.7 | Immunoblot analysis and immunoprecipitations

KS cells were grown in 6-cm dishes to 70–80% confluence and exposed to treatments as indicated. The cells were harvested in cold phosphate-buffered saline (PBS) and then subjected to total/nuclear/cytoplasmic proteins extraction as previously described.¹⁹ An equal amount of proteins was separated by SDS/PAGE electrophoresis and immunoblotted with primary antibodies directed against Caspase 3, PARP1, BCN1, LC3B, SQSTM1, p-Bcl-2, Bcl-2, p75^{NTR}, EGR1, GR, SP1, AP2 α , NF1, PI3K, p-AKT, tot-AKT, p-mTOR, tot-mTOR, p70S6K, p-ERK1/2, tot-ERK1/2, p-JNK, tot-JNK, PTEN, GAPDH and Lamin B (Santa Cruz Biotechnology, Santa Cruz, CA). All antibodies were detected with horseradish peroxidase-conjugated goat anti-rabbit, anti-mouse or anti-goat antibodies (Santa Cruz Biotechnology, Santa Cruz, CA). GAPDH and Lamin B were used as loading controls for cytosolic and nuclear extracts, respectively. LC3B-II was normalized with respect to LC3B-I and GAPDH. Phosphorylated proteins were normalized to respective totals and GAPDH.

For co-immunoprecipitation experiments, it has been used 1mg of extracts protein and 2 mg of BCN1 antibody overnight, followed by protein A/G precipitation. Equal amounts of cell extracts and coimmunoprecipitated protein were subjected to SDS polyacrylamide gel electrophoresis, as described earlier.¹⁹ Membranes were probed with anti-BCN1 and anti-Bcl-2 antibodies. The bands of interest were quantified by Image J densitometry scanning program.

2.8 | Flow cytometric cell cycle analysis

To determine cell cycle distribution analysis, KS cells were harvested by trypsinization, fixed and stained with propidium iodide (100 μ g/ml) after treatment with RNase A (20 μ g/ml). The DNA content was measured using a FACScan flow cytometer (Becton Dickinson, Mountain View, CA, USA) and the data acquired using CellQuest software. Cell cycle profiles were determined using Mod-Fit LT.

2.9 | Immunofluorescence assay

For immunofluorescence assay (IF), KS cells, grown on glass coverslips, were treated with Rapa and/or BAF. After treatment, cells were fixed in 4% paraformaldehyde for 20 min. Subsequently, cells were permeabilized with 0.2% Triton X-100, blocked with 0.5% BSA, and then incubated overnight with antibody anti-SQSTM1 (Santa Cruz Biotechnology, Santa Cruz, CA). The next day, the slides were incubated with secondary antibody anti-mouse IgG FITC-conjugated (Invitrogen, Carlsbad, CA, USA) for 1h at RT in the dark. The nuclei were counterstained with DAPI. Negative cells were incubated replacing the anti-SQSTM1 antibodies with normal mouse IgG utilized as the negative control (NC). The cellular localization of protein was visualized using a fluorescence microscope with $\times 20$ magnification.

2.10 | Transfection assay

KS cells were transfected using Lipofectamine 2000 (Invitrogen, Carlsbad, CA, USA), according to manufacturer's instructions, in a complete medium without penicillin/streptomycin with 100 nM of Validated Stealth p75^{NTR} targeted for the human p75^{NTR} mRNA sequence RNAi (Invitrogen, ID:1299001), or with a negative control RNAi (Invitrogen, 452001) that does not match with any currently known human mRNA (scrambled siRNA). The efficiency of knock-down for each gene and the negative control was determined by Western blot analyses (data not shown). After 24h with the respective siRNA complexes, the cells were treated as indicated.

Functional studies were performed in KS cells transfected for 24 h with wild-type p75^{NTR} promoter (p75^{NTR}-900 + 100, WT) and its deletion constructs (p75^{NTR}-164 + 100, p75^{NTR}-315 + 100, p75^{NTR}-41 + 100), concomitant with 5 ng of pRLCMV (Promega, Madison, Wisconsin, USA), which expresses Renilla luciferase enzymatically distinguishable from firefly luciferase by the strong cytomegalovirus enhancer/promoter, using the Fugen 6 reagent (Promega, Madison, Wisconsin, USA). Then, KS cells were treated as reported. Firefly and Renilla luciferase activities were measured using a dual-luciferase kit (Promega, Madison, Wisconsin, USA). The firefly luciferase values for each sample were normalized based on the transfection efficiency measured by Renilla luciferase activity.

2.11 | Real-time RT-PCR assay

KS cells were grown in 10 cm dishes to 70%–80% confluence and exposed to treatments as indicated. Total cellular RNA was extracted using TRIZOL reagent (Invitrogen, Carlsbad, CA, USA) as suggested by the manufacturer. The purity and integrity of the RNA were confirmed both spectroscopically and electrophoretically. RNA (1 μ g/sample) was reverse transcribed to give complementary DNA (cDNA) using the High capacity cDNA Archive Kit (Applied

Biosystems, Milan, Italy). Analysis of p75NTR, BCN1, LC3B and GAPDH gene expression was performed by qRT-PCR using primers as previously described.¹² Each sample was normalized on its GAPDH mRNA content.

2.12 | Chromatin immunoprecipitation (ChIP) assay

For the ChIP assay, KS cells were treated with Rapa for 6h or pre-incubated with Mithramycin A (100 nM) for 1h where required. Thereafter, the cells were subjected to the ChIP assay as described previously.¹² Chromatin was immunoprecipitated with anti-EGR1 or anti-RNA PolII antibodies (Santa Cruz Biotechnology, Santa Cruz, CA). Purified DNA (0.5 ml) was used as a template for real-time PCR detection using primers flanking the EGR1 site sequence present in the human p75NTR promoter: Fw: 5'-GGACCGAGCTGGAAGTCG-3' and Rv: 5'-GCTAACACTCACCCCGAGAA-3'. The results were normalized in comparison with the input DNA.

2.13 | Statistical analysis

All experiments were performed in at least triplicate per treatment and repeated in three independent experiments, we showed the results as mean \pm SD. Data were analysed by Student's t test using the GraphPad Prism 4 software program. Data from the Immunohistochemistry and Confocal Laser Scanning Microscopy were expressed as the mean \pm SD and differences between groups were analysed by paired t test analysis. A *p*-value < 0.05 was considered statistically significant.

3 | RESULTS

3.1 | Cutaneous KS lesions express high levels of autophagic markers

To evaluate the activation of autophagy in KS, we measured, by immunofluorescence analysis, the expression level of major autophagic markers (BCN1, LC3B and SQSTM1) on both skin biopsies of normal perilesional skin (controls) and histologically confirmed KS lesions. Interestingly, BCN1 and LC3B resulted upregulated, while SQSTM1 was downregulated in KS lesions compared to the dermis area of the normal skin, indicating an activation of the autophagic process (Figure 1A-C).

3.2 | Rapamycin affects proliferation of KS cells by increasing the autophagic process

To assess whether Rapa was able to affect KS cells' proliferation, we measured cell viability, by using MTT assay, after 48h treatment

with increasing doses of Rapa (0.1-1-5-10-20-50-75-100-125-150 ng/ml). Results showed that Rapa-induced anti-proliferative effects in a dose-dependent manner (Figure 2A). The half-maximal inhibitory concentration (IC50) was 41.1 ng/ml; this dose was used for all subsequent experiments. Subsequently, to evaluate the impact of Rapa on KS cell growth, we performed the soft agar assay in which KS cells were exposed to Rapa for 14 days. After this period, the number of colonies >50mm diameter were counted. As expected, Rapa significantly reduced the number of colonies (Figure 2B).

To better investigate the mechanism by which Rapa reduced KS cell viability, we evaluated, by Western blotting, the level of protein expression of some pro-apoptotic biomarkers. Results of protein analysis revealed that PARP1 and Caspase 3 cleavage were not changed by treatment for 48 h with Rapa (Figure 2C). Moreover, flow cytometric cell cycle analysis in KS cells treated as above reported, revealed that 18h exposure to Rapa was able to induce a cell cycle arrest in the G0/G1 phase, concomitantly with a low percentage of cells in the G1/S phase (Figure S1 upper panel). As expected, the percentage of apoptotic cells was not significant. Comparable results were observed in cells treated with Rapa for 48h, confirming the absence of apoptotic events also in the long-term experimental treatment (Figure S1 lower panel). Altogether these data underlined that in our experimental model, Rapa exerts its inhibitory effect on KS cell viability without influencing apoptosis.

To explore whether the inhibitory effects of Rapa on cellular viability was due to an enhancement of the autophagic process, we measured the level of several pro-autophagic proteins by Western blot analysis in KS cells exposed to Rapa for 6 h. As showed in Figure 2D (left panel), Rapa upregulated BCN1, enhanced the conversion of LC3B-I in the active cleaved form LC3B-II and reduced the content of SQSTM1, underlying the positive effect of Rapa on the autophagic flux. All the above-mentioned effects were abrogated in cells pretreated for 1h with BAF, a classical autophagy inhibitor (Figure 2D right panel). Upon BAF pretreatment, we did not observe a significant amount in LC3-II levels. This could be due to drawbacks in Western blot method used for measuring endogenous LC3-II and because when cells are treated with unsaturating concentrations of Chloroquine or BAF, LC3 lipidation would be insufficiently blocked, leading to a lack of increase of LC3-II levels.^{20,21}

Furthermore, MTT data, performed in cells treated with Rapa and BAF for 48h, showed that the Rapa-induced reduction of cellular viability was reversed when autophagy was abrogated (Figure 2E), suggesting that the anti-proliferative effects exerted by Rapa in KS cells occurred by increasing the autophagic process. Interestingly, our results showed that Rapa exposure, in addition to the upregulation of BCN1 levels, promoted Bcl-2 phosphorylation, enhancing the autophagic process (Figure S2 left panel). To further confirm the autophagy activation, we performed a co-immunoprecipitation assay using a primary antibody direct against BCN1 protein, demonstrating that in cells treated with Rapa for 6h, the complex BCN1/Bcl-2 resulted significantly reduced (Figure S2 right panel).

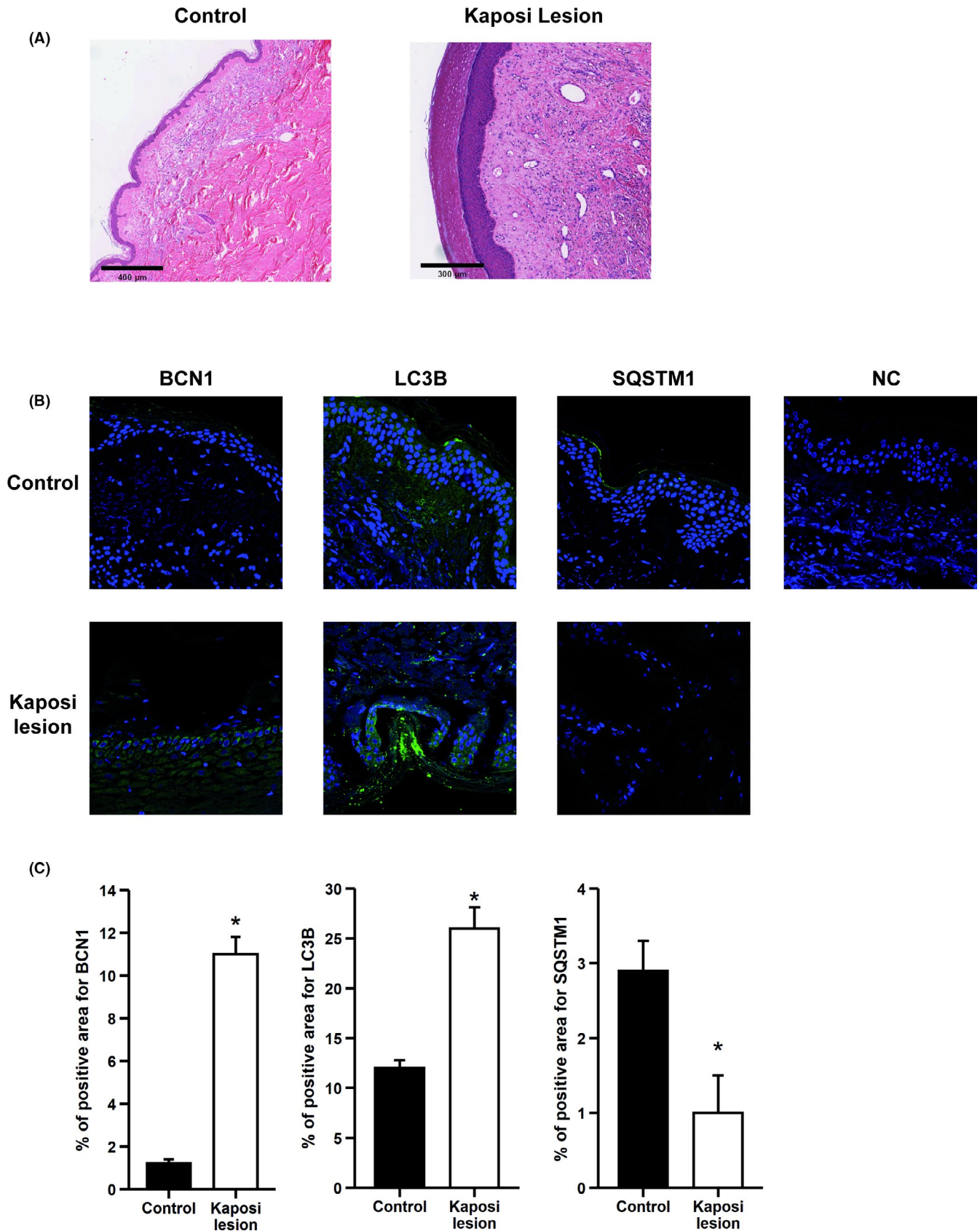


FIGURE 1 Autophagic markers expression on KS lesions: (A) Representative images of haematoxylin and eosin and (B) immunofluorescence analysis of BCN1, LC3B and SQSTM1 on normal perilesional skin (Control) and KS lesions. NC (negative control). (C) Quantification of specific staining for BCN1, LC3B and SQSTM1. * $p < 0.05$.

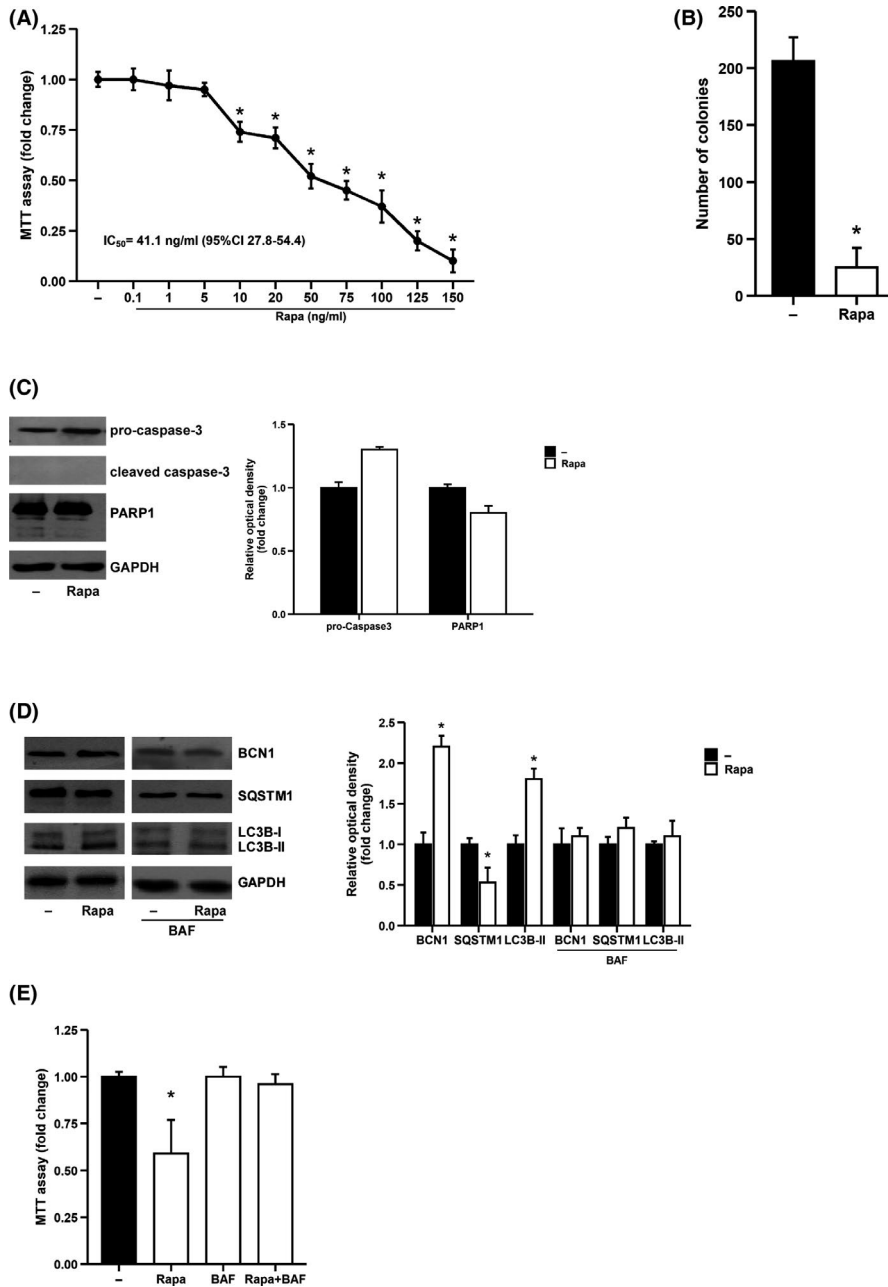


FIGURE 2 Rapamycin reduces KS cells proliferation via autophagy activation: (A) MTT assays of KS cells untreated (-) or treated with increasing doses of Rapa. (B) Soft-agar growth assay in KS cells untreated (-) or treated with Rapa. (C) Representative immunoblot of Caspase 3 and PARP1; (D) Protein expression of BCN1, SQSTM1, LC3B and (E) MTT assay, in KS cells untreated (-) or treated with Rapa with or without pretreatment with BAF. * $p < 0.05$ vs untreated cells (-)

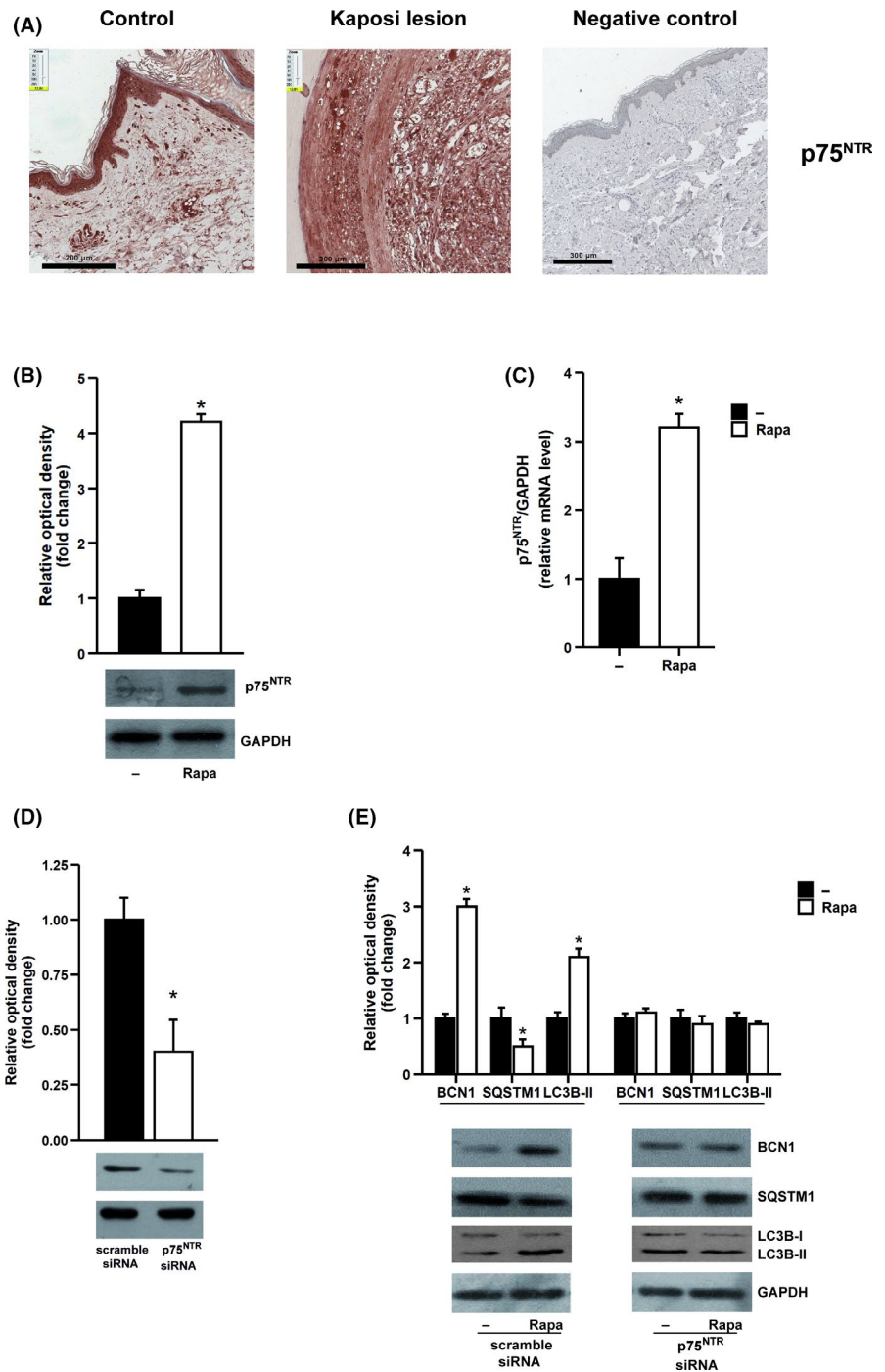
3.3 | Rapamycin exposure promotes autophagy via p75^{NTR} receptor in KS cells

As immunohistochemistry revealed a higher expression of the p75^{NTR} in KS tissue compared to normal perilesional skin (Figure 3A), we investigated whether the in vitro administration of Rapa was able to modulate this receptor in KS cell lines. Firstly, we demonstrated that Rapa exposure significantly increased p75^{NTR} protein and mRNA expression compared to untreated cells (Figure 3B-C). Interestingly, we observed that in KS cells transfected with siRNA p75^{NTR} for 48 h (Figure 3D), Rapa exposure for 6 h did not promote any change in the protein level of BCN1, SQSTM1 and the LC3B-I to LC3B-II conversion (Figure 3E). These data strongly suggested a pivotal role of p75^{NTR} in mediating Rapa-induced autophagy.

3.4 | Rapamycin transactivates p75^{NTR} promoter via EGR1, promoting autophagy in KS cells

To explore whether the upregulation of p75^{NTR} following Rapa treatment relayed on transcriptional mechanisms, we used a luciferase reporter plasmid containing the wild-type p75^{NTR} promoter region (from -900 to +100 base pairs), and with its deletion constructs (p75^{NTR} -164 + 100, p75^{NTR} -315 + 100, p75^{NTR} -41 + 100), each one lacking multiple consensus sites (Figure S3 A). After 24 h, transfected cells were treated as reported and then luciferase activity was measured. Results showed that Rapa activated p75^{NTR} promoter (Figure 4A) and the responsiveness to this agent was still maintained using the p75^{NTR} -41 + 100 (Figure S3B), suggesting that one of the five consensus sites contained in the last construct (EGR1, GR, SP1, AP2 α and NF1) was involved in the transactivation of the p75^{NTR}

FIGURE 3 Rapamycin enhances autophagy via p75^{NTR} (A) Immunohistochemistry of p75^{NTR} on normal perilesional skin (Control), KS lesions and Negative Control. (B) Protein and (C) mRNA expression of p75^{NTR} of KS cells untreated (-) or treated with Rapa. (D) p75^{NTR} protein level from KS cells transfected for 48h with scramble siRNA and p75^{NTR} siRNA (E) Protein levels of BCN1, SQSTM1 and LC3B in KS cells transfected with scrambled or p75^{NTR} siRNA and then treated with Rapa. **p* < 0.05 vs untreated cells (-)



promoter. Therefore, we explored the cytosolic and nuclear modulation of the above-mentioned transcription factors in KS cells treated for 6h with Rapa. As showed in Figure 4B, the high nuclear content of EGR1 was evident upon treatment; conversely, the modulation of the other four transcription factors resulted not significant (data not shown). Interestingly, we observed that the nuclear translocation of EGR1 induced by Rapa was reversed in cells knocked down for the p75^{NTR} gene (Figure 4B left panel).

To confirm the involvement of EGR1 in the transcriptional activation of p75^{NTR} promoter, we performed a ChIP assay. Protein-chromatin complexes obtained from KS cells treated or untreated with Rapa for 6h were immunoprecipitated using specific antibodies

against EGR1 and RNA polymerase II proteins. The precipitated DNA was then quantified using real-time PCR with primers flanking the EGR1 binding elements in the p75^{NTR} promoter region. As showed in Figure 4B (left panel), Rapa increased the recruitment of EGR1 on its responsive element sited on p75^{NTR} promoter concomitantly with a higher association of RNA polymerase II (Figure 4B right panel). As reported in Figure 4B, the increased recruitment of EGR1 and RNA polymerase II observed upon Rapa treatment was abrogated in KS cells pretreated for 30' with Mithramycin A, a GC-rich inhibitor that displaces EGR1 binding to DNA. Taken together, our results revealed a potential role of EGR1 as a candidate transcriptional regulator of autophagy via p75^{NTR} in KS cells after mTOR-I treatment.

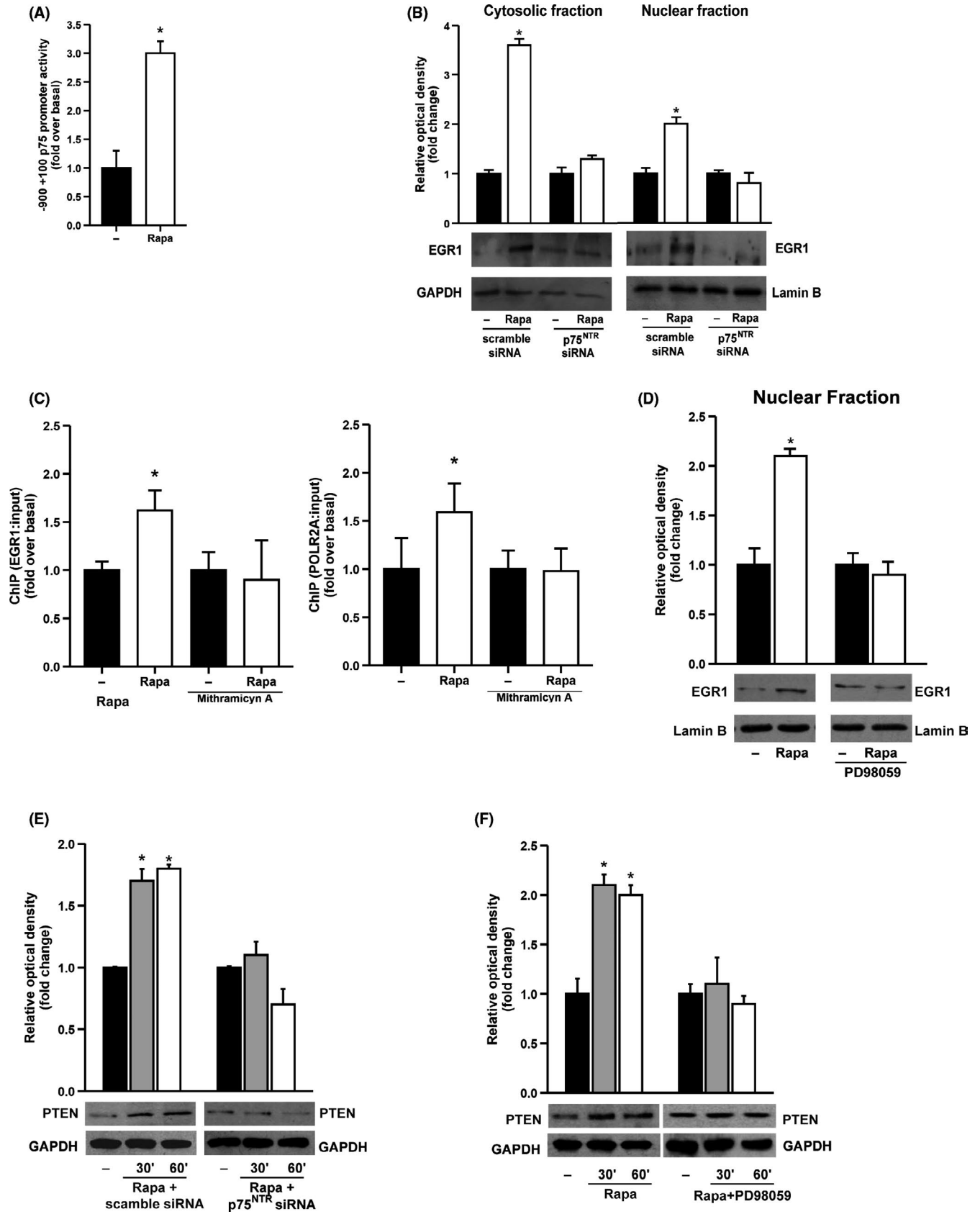


FIGURE 4 EGR1 transcriptionally activates p75^{NTR} and its downstream signalling, promoting autophagy and PTEN/PI3K/Akt/mTOR pathway modulation: (A) Luciferase activity of KS cells transfected with WT p75^{NTR} promoter in KS cells untreated (-) or treated with Rapa. (B) Cytosolic and nuclear translocation of EGR1 in KS transfected with scrambled and p75^{NTR} siRNA and then treated with Rapa (C) Real-time PCR from KS cells treated with Rapa and Mithramycin A alone or in combination and then subjected to ChIP assay as indicated. The precleared chromatin was immunoprecipitated with anti-EGR1 and anti-POLR2A, antibodies. (D) EGR1 nuclear content in KS cells untreated (-) or treated with Rapa for 6h, with or without pretreatment with PD98059 (E) Protein levels of PTEN in KS cells transfected with scrambled or p75^{NTR} siRNA or (F) with or without pretreatment with PD98059 and then treated with Rapa, for 30' and 60'. **p* < 0.05 vs untreated cells (-)

3.5 | In KS cells exposed to RAPA, p75^{NTR} downstream signalling activation modulates PTEN/PI3K/Akt/mTOR pathway, via EGR1

As expected, time course assay performed in KS cells shortly exposed to Rapa, showed a downregulation of the PI3K/Akt/mTOR axis, as well as of the ribosomal protein P70S6 kinase; in the same experimental conditions, by evaluating the downstream signalling of p75^{NTR}, we observed increased phosphorylation of ERK1/2; conversely, the JNK pathway was not activated (Figure S4A). Of interest, the nuclear translocation of EGR1 was not observed in cells pretreated for 1h with the ERK1/2 inhibitor PD98059 (Figure S4B), suggesting that the enhanced p-ERK1/2 leads to an increased nuclear content of EGR1 (Figure 4D). Finally, based on data that support that PTEN has a major role in regulating the PI3K/Akt/mTOR signalling pathway and it plays an essential role in the development and progression of human cancers, including KS,^{22,23} we measured its level in KS cells after short-time exposure to Rapa, as reported. Interestingly, we observed an upregulation of PTEN expression (Figure 4E left panel) which was reversed in p75^{NTR} knock-down cells (Figure 4E right panel), as well as in cells pretreated with PD98059 (Figure 4F), highlighting the role of p75^{NTR} as a modulator of PTEN via ERK1/2 pathway activation Rapa-induced.

4 | DISCUSSION

Our study, using several biomolecular methodologies, showed that Rapa was able to hence autophagy in KS cells, leading to cancer cell death. This finding, although already demonstrated in other cancer cell types,²⁴ has been not reported in this common postkidney transplant malignancy yet and it may contribute to better elucidate the antineoplastic mechanisms exerted by Rapa in KS. Indeed, many authors demonstrated that in kidney renal recipients the switch from calcineurin-inhibitors to the mTOR inhibitors, as Rapa, can reduce the risk of skin cancer and promote the clinical remission of KS lesions.^{6,7} The recent multicentre retrospective cohort study conducted by Deylon J et al. confirmed that a reduction of immunosuppression associated with conversion to mTORi was effective to control KS in most patients (responses at 6 months to first-line treatment, classified as complete response or partial response, of approximately 80%).²⁵ In this large clinical study, there were no data regarding mTOR inhibitors systemic side effects which occurred in the cohort of KS patients. However, as other immunosuppressive drugs, mTORi may induce the development of several adverse

effects (eg pulmonary toxicity, haematological disorders, dismetabolism and lymphedema) that need to be early diagnosed and treated to avoid severe illness in renal transplant patients. All these side effects are most of the time reversible and dose related.²⁶

The role of autophagy in cancer progression is very debated, as it can either counteract or promote cell death, depending on the different cancer cell types and conditions.^{10,11} In agreement with the report by White et al.,²⁷ our immunofluorescence assays revealed an increased expression of the main autophagic markers in skin biopsies of KS lesions, suggesting that in this cancer the higher basal autophagy may have a role in KS cell survival.

Interestingly, our *in vitro* results demonstrated that in KS cells, Rapa promotes autophagy cell death in absence of apoptosis and that the inhibition of autophagy abrogates the reduction of cell viability, suggesting that the increase of basal autophagic flux may represent the key anti-proliferative mechanism of Rapa. These findings are consistent with the recently proposed requirements for the definition of autophagy cell death, that is increased autophagic flux, cell death without the evident involvement of apoptosis and no cell death following inhibition of autophagy.²⁸

Concomitantly, immunoprecipitation studies showed that Rapa exposure significantly reduced the complex BCN1/Bcl-2, sustaining the autophagy induction. The latter finding emphasized the apoptosis-autophagy interaction, which has been deeply described, although their relationship is not well understood. Interestingly, it has been proposed that the functional and physical interaction between the antiapoptotic protein Bcl-2 and BCN1, is responsible for the switch between these two cell death mechanisms, as the dissociation of BCN1 from Bcl-2 is essential for its autophagic activity.²⁸⁻³¹

The most interesting finding emerging from our results is the central role of p75^{NTR} in the Rapa-induced autophagic process. This neurotrophic receptor is a part of the tumour necrosis factor receptor superfamily, which is expressed by KS cells, even if its role in this cancer is not been elucidated yet.³² Some authors reported that p75^{NTR} activation promotes pro-apoptotic or autophagic events, in neuronal and non-neuronal cells.^{12,33,34} Besides, accumulating *in vitro* and *in vivo* studies reported that p75^{NTR} plays an important role in cancer cells, as promoting tumour cell survival and invasion or decreasing cell survival.³⁵⁻³⁸

In our cellular model, we observed that the upregulation of the main autophagic markers Rapa-induced resulted abrogated in p75^{NTR} knocked-down cells and that the activation of p75^{NTR} occurred in a transcriptional dependent manner, via the transcription factor EGR1.

EGR1 is involved in many cellular functions, including apoptosis, proliferation, angiogenesis, migration, and cell differentiation,³⁹ which antineoplastic effects are poorly described, but, as recently demonstrated by Dai et al, EGR1 hyper-expression in Kaposi's sarcoma-associated herpesvirus (HHV8) may promote autophagy, through the regulation of LC3B expression, and it was required for Sphingosine Kinase 2 Inhibitor-induced autophagic tumoral cells death.⁴⁰ Sustained expression of EGR1 by recombinant adenoviruses in endothelial cells leads to a specific induction of compelling feedback inhibitory mechanisms, including strong upregulation of transcriptional repressors, negative cell cycle check-point effectors and several pro-apoptotic genes.⁴¹ However, in other cellular models, EGR1 exerted opposite effects. In particular, as recently reported by Yoon YJ et al, its activation in endothelial cells was involved in the angiogenic activity of colorectal cancer cell-derived extracellular vesicles.⁴²

Additionally, we found that the activation Rapa-induced of p75^{NTR} downstream signalling, p-ERK1/2, promotes the upregulation of PTEN, the tumour suppressor that modulates PI3K/Akt/mTOR pathway, crucial signalling that, when inhibited by Rapa, may reduce KS tumour growth.⁴³ Interestingly, we observed that in cells p75^{NTR} knocked-down or pretreated with ERK pathway inhibitor, the upregulation of both EGR1 and PTEN resulted abrogated. These findings could reflect the ability of the "mutual modulation" between p75^{NTR} and EGR1 induced by Rapa treatment to modulate PTEN, inducing cell growth-suppressing effect and sustaining the autophagic cell death.^{44,45}

Collectively, our data suggest that the increase of the autophagic flux promoted by Rapa in KS cells, leading to tumour regression, occurs through the p75^{NTR} pathway activation which, in turn, triggers a feedback positive loop with EGR1, further sustaining the autophagic cell death.

However, future studies should be performed to confirm our assumptions and to validate p75^{NTR} as a new predictive biomarker of the response of Kaposi's Sarcoma to mTOR inhibitors treatment in kidney transplant recipients.

ACKNOWLEDGMENTS

None.

CONFLICT OF INTEREST

The authors declare no conflict of interest.

AUTHOR CONTRIBUTIONS

Anna Perri designed the study and wrote the manuscript. Simona Lupinacci, Giuseppina Totoda, Donatella Vizza and Antonella La Russa performed the in vitro experiments. Gianpaolo Tessari performed the skin biopsies of KS lesions and normal-appearing perilesional skin. Paola Pontrelli and Chiara Divella performed the immunohistochemical and immunofluorescence analysis on Skin biopsies specimens. Danilo Lofaro analysed the data. Gianluigi Zaza, Giovanni Stallone and Renzo Bonofiglio reviewed the manuscript. All authors have read and agreed to the published version of the manuscript.

ORCID

Anna Perri  <https://orcid.org/0000-0002-2852-0919>

REFERENCES

1. Lebbe C, Legendre C, Frances C. Kaposi sarcoma in transplantation. *Transplant Rev*. 2008;22(4):252-261.
2. Riva G, Luppi M, Barozzi P, Forghieri F, Potenza L. How I treat HHV8/KSHV-related diseases in posttransplant patients. *Blood*. 2012;120(20):4150-4159.
3. Vajdic CM, McDonald SP, McCredie MRE, et al. Cancer incidence before and after kidney transplantation. *JAMA*. 2006;296(23):2823-2831.
4. Hojo M, Morimoto T, Maluccio M, et al. Cyclosporine induces cancer progression by a cell-autonomous mechanism. *Nature*. 1999;397(6719):530-534.
5. Maluccio M, Sharma V, Lagman M, et al. Tacrolimus enhances transforming growth factor-beta1 expression and promotes tumor progression. *Transplantation*. 2003;76(3):597-602.
6. Stallone G, Schena A, Infante B, et al. Sirolimus for Kaposi's sarcoma in renal-transplant recipients. *N Engl J Med*. 2005;352(13):1317-1323.
7. Yaich S, Charfeddine K, Zaghdane S, et al. Sirolimus for the treatment of Kaposi sarcoma after renal transplantation: a series of 10 cases. *Transplant Proc*. 2012;44(9):2824-2826.
8. Liu B, Bao JK, Yang JM, Cheng Y. Targeting autophagic pathways for cancer drug discovery. *Chin J Cancer*. 2013;32(3):113-120.
9. Klionsky DJ, Abdelmohsen K, Abe A, et al. Guidelines for the use and interpretation of assays for monitoring autophagy (3rd edition). *Autophagy*. 2016;12(1):1-222.
10. Baehrecke EH. Autophagy: dual roles in life and death? *Nat Rev Mol Cell Biol*. 2005;6(6):505-510.
11. Shanware NP, Bray K, Abraham RT. The PI3K, metabolic, and autophagy networks: interactive partners in cellular health and disease. *Annu Rev Pharmacol Toxicol*. 2013;53:89-106.
12. Vizza D, Perri A, Totoda G, et al. Rapamycin-induced autophagy protects proximal tubular renal cells against proteinuric damage through the transcriptional activation of the nerve growth factor receptor NGFR. *Autophagy*. 2018;14(6):1028-1042.
13. Tomellini E, Lagadec C, Polakowska R, Le Bourhis X. Role of p75 neurotrophin receptor in stem cell biology: more than just a marker. *Cell Mol Life Sci*. 2014;71(13):2467-2481.
14. Chopin V, Lagadec C, Toillon RA, Le Bourhis X. Neurotrophin signaling in cancer stem cells. *Cell Mol Life Sci*. 2016;73(9):1859-1870.
15. Pontrelli P, Oranger A, Barozzino M, et al. Deregulation of autophagy under hyperglycemic conditions is dependent on increased lysine 63 ubiquitination: a candidate mechanism in the progression of diabetic nephropathy. *J Mol Med*. 2018;96(7):645-659.
16. Albin A, Paglieri I, Orengo G, et al. The beta-core fragment of human chorionic gonadotrophin inhibits growth of Kaposi's sarcoma-derived cells and a new immortalized Kaposi's sarcoma cell line. *Aids*. 1997;11(6):713-721.
17. Stallone G, Infante B, Pontrelli P, et al. ID2-VEGF-related pathways in the pathogenesis of Kaposi's sarcoma: a link disrupted by rapamycin. *Am J Transplant*. 2009;9(3):558-566.
18. Lupinacci S, Perri A, Totoda G, et al. Olive leaf extract counteracts epithelial to mesenchymal transition process induced by peritoneal dialysis, through the inhibition of TGFbeta1 signaling. *Cell Biol Toxicol*. 2019;35(2):95-109.
19. Vizza D, Perri A, Lofaro D, et al. Exposure to nerve growth factor worsens nephrotoxic effect induced by Cyclosporine A in HK-2 cells. *PLoS One*. 2013;8(11):e80113.
20. Ni H-M, Bockus A, Wozniak AL, et al. Dissecting the dynamic turnover of GFP-LC3 in the autolysosome. *Autophagy*. 2011;7(2):188-204.

21. Mizushima N, Yoshimori T, Levine B. Methods in mammalian autophagy research. *Cell*. 2010;140(3):313-326.
22. Hernández-Sierra A, Rovira J, Petit A, et al. Role of HHV-8 and mTOR pathway in post-transplant Kaposi sarcoma staging. *Transpl Int*. 2016;29(9):1008-1016.
23. Xu D, Yao Y, Jiang X, Lu L, Dai W. Regulation of PTEN stability and activity by Plk3. *J Biol Chem*. 2010;285(51):39935-39942.
24. Zaza G, Granata S, Caletti C, Signorini L, Stallone G, Lupo A. mTOR inhibition role in cellular mechanisms. *Transplantation*. 2018;102(2S):S3-S16.
25. Delyon J, Rabate C, Euvrard S, et al. Management of Kaposi sarcoma after solid organ transplantation: A European retrospective study. *J Am Acad Dermatol*. 2019;81(2):448-455.
26. Zaza G, Tomei P, Ria P, Granata S, Boschiero L, Lupo A. Systemic and nonrenal adverse effects occurring in renal transplant patients treated with mTOR inhibitors. *Clin Dev Immunol*. 2013;2013:403280.
27. White E. Deconvoluting the context-dependent role for autophagy in cancer. *Nat Rev Cancer*. 2012;12(6):401-410.
28. Liu JJ, Lin M, Yu JY, Liu B, Bao JK. Targeting apoptotic and autophagic pathways for cancer therapeutics. *Cancer Lett*. 2011;300(2):105-114.
29. Pattinre S, Tassa A, Qu X, et al. Bcl-2 antiapoptotic proteins inhibit Beclin 1-dependent autophagy. *Cell*. 2005;122(6):927-939.
30. Maiuri MC, Ciriollo A, Kroemer G. Crosstalk between apoptosis and autophagy within the Beclin 1 interactome. *EMBO J*. 2010;29(3):515-516.
31. Chang NC, Nguyen M, Germain M, Shore GC. Antagonism of Beclin 1-dependent autophagy by BCL-2 at the endoplasmic reticulum requires NAF-1. *EMBO J*. 2010;29(3):606-618.
32. Pica F, Volpi A, Barillari G, et al. Detection of high nerve growth factor serum levels in AIDS-related and -unrelated Kaposi's sarcoma patients. *Aids*. 1998;12(15):2025-2029.
33. Liepinsh E, Ilag LL, Otting G, Ibanez CF. NMR structure of the death domain of the p75 neurotrophin receptor. *EMBO J*. 1997;16(16):4999-5005.
34. Florez-McClure ML, Linseman DA, Chu CT, et al. The p75 neurotrophin receptor can induce autophagy and death of cerebellar Purkinje neurons. *J Neurosci*. 2004;24(19):4498-4509.
35. Dang C, Zhang Y, Ma Q, Shimahara Y. Expression of nerve growth factor receptors is correlated with progression and prognosis of human pancreatic cancer. *J Gastroenterol Hepatol*. 2006;21(5):850-858.
36. Faulkner S, Jobling P, Rowe CW, et al. Neurotrophin receptors TrkA, p75(NTR), and sortilin are increased and targetable in thyroid cancer. *Am J Pathol*. 2018;188(1):229-241.
37. Johnston ALM, Lun X, Rahn JJ, et al. The p75 neurotrophin receptor is a central regulator of glioma invasion. *PLoS Biol*. 2007;5(8):e212.
38. Verbeke S, Meignan S, Lagadec C, et al. Overexpression of p75(NTR) increases survival of breast cancer cells through p21(waf1). *Cell Signal*. 2010;22(12):1864-1873.
39. Li TT, Liu MR, Pei DS. Friend or foe, the role of EGR-1 in cancer. *Med Oncol*. 2019;37(1):7.
40. Dai L, Bai A, Smith CD, Rodriguez PC, Yu F, Qin Z. ABC294640, a novel sphingosine kinase 2 inhibitor, induces oncogenic virus-infected cell autophagic death and represses tumor growth. *Mol Cancer Ther*. 2017;16(12):2724-2734.
41. Lucerna M, Pomyje J, Mechtcheriakova D, et al. Sustained expression of early growth response protein-1 blocks angiogenesis and tumor growth. *Cancer Res*. 2006;66(13):6708-6713.
42. Yoon YJ, Kim D-K, Yoon CM, et al. Egr-1 activation by cancer-derived extracellular vesicles promotes endothelial cell migration via ERK1/2 and JNK signaling pathways. *PLoS One*. 2014;9(12):e115170.
43. Granata S, Dalla Gassa A, Carraro A, et al. Sirolimus and everolimus pathway: reviewing candidate genes influencing their intracellular effects. *Int J Mol Sci*. 2016;17(5):735.
44. Marino M, Acconcia F, Trentalance A. Biphasic estradiol-induced AKT phosphorylation is modulated by PTEN via MAP kinase in HepG2 cells. *Mol Biol Cell*. 2003;14(6):2583-2591.
45. Virolle T, Adamson ED, Baron V, et al. The Egr-1 transcription factor directly activates PTEN during irradiation-induced signalling. *Nat Cell Biol*. 2001;3(12):1124-1128.

SUPPORTING INFORMATION

Additional supporting information may be found online in the Supporting Information section.

FIGURE S1. Cell cycle analysis in KS cells untreated (-) or treated with Rapa

FIGURE S2. (A) Immunoblots of BCN1, p-Bcl-2, and Bcl-2 of KS cells untreated (-) or treated with Rapa. (B) Protein extracts of KS cells untreated (-) or treated with Rapa immunoprecipitated using anti-BCN1 (IP: BCN1) antibody. * $p < 0.05$ vs untreated cells (-).

FIGURE S3. (A) Schematic representation of the WT human p75^{NTR} and its deletion constructs (B) Luciferase activity of KS cells transfected with WT p75^{NTR} promoter deletion constructs and treated or not with Rapa. * $p < 0.05$ vs untreated cells (-).

FIGURE S4. (A) Levels of phosphorylated and total Akt, mTOR, ERK1/2, and JNK, PI3K and P70S6K in KS cells untreated (-) or treated with Rapa for 30' and 60'. (B) Levels of p-ERK1/2 in KS cells untreated (-) or treated with Rapa for 30' and 60', with or without pretreatment with PD98059. * $p < 0.05$ vs untreated cells (-).

How to cite this article: Lupinacci S, Perri A, Toteda G, et al. Rapamycin promotes autophagy cell death of Kaposi's sarcoma cells through P75NTR activation. *Exp Dermatol*. 2022;31:143-153. <https://doi.org/10.1111/exd.14438>